JOURNAL OF GEOPHYSICAL RESEARCH, VOL. 86, NO. A10, PAGES 8833-8841, SEPTEMBER 30, 1981

Parametric Interaction and Spatial Collapse of Beam-Driven Langmuir Waves in the Solar Wind

D. A. GURNETT,[1,2] J. E. MAGGS,[3] D. L. GALLAGHER,[1]
W. S. KURTH,[1] AND F. L. SCARF[4]

This paper presents observations of the parametric decay and spatial collapse of Langmuir waves driven by an electron beam streaming into the solar wind from the Jovian bow shock. High-resolution frequency-time spectrograms from Voyager 1 and 2 show that long wavelength Langmuir waves upstream of the bow shock are very effectively converted into short wavelength Langmuir waves which are no longer in resonance with the beam. This conversion is shown to be the result of a nonlinear interaction involving the beam-driven pump, a sideband emission and a low level of ion-acoustic turbulence which always appears to be present in the solar wind. The onset of the interaction occurs at about the time that the amplitude of the pump wave saturates, which indicates that parametric processes are probably playing an important role in stabilizing the electron beam. Detailed examination of the electric field waveforms shows that the beam-driven Langmuir wave emission breaks up into a very complex sideband structure with both positive and negative Doppler shifts. Positive frequency shifts correspond to waves propagating away from the sun and negative frequency shifts correspond to waves propagating toward the sun. In some cases the sideband emissions consist of isolated wave packets with very short durations, sometimes lasting only a few msec. These short duration bursts, which are usually very intense, are thought to consist of envelope solitons which have collapsed down to spatial scales of only a few Debye lengths.

1. INTRODUCTION

In this paper we describe what are believed to be the first observations of parametric interactions involving Langmuir waves driven by an electron beam in the solar wind. When an electron beam of sufficient intensity is present in a plasma it is well known that exponentially growing electrostatic oscillations, called Langmuir waves or electron plasma oscillations, are generated by a mechanism known as the two-stream instability [*Bohm and Gross,* 1949]. The nonlinear effects which occur when these waves reach large amplitudes are of considerable general interest and have important implications for the propagation of beams in plasmas. In the absence of nonlinear effects the waves quickly grow to such large amplitudes that the beam would be completely disrupted by resonant wave-particle interactions after traveling only a short distance. In both space and laboratory plasmas ample evidence exists that nonlinear processes somehow limit these disruptive effects, since electron beams are often observed to propagate large distances, as for example in the case of energetic solar flare electrons which travel from the sun to the Earth without appreciable loss of energy [*Lin,* 1970].

Several attempts have been made to account for the electron beam stabilization by considering various nonlinear interactions which transfer energy from the resonant Langmuir waves to other waves not in resonance with the beam. The interactions which have been proposed include scattering by thermal fluctuations [*Kaplan and Tsytovich,* 1968], parametric instabilities [*Papadopoulos et al.,* 1974; *Fried et al.,* 1976; *Bardwell and Goldman,* 1976; *Goldstein et al.,* 1979; *Freund and Papadopoulos,* 1980], and the related nonlinear phenomenon of soliton collapse [*Zakharov,* 1972; *Galeev et al.,* 1975; *Nicholson et al.,* 1978; *Smith et al.,* 1979; *Goldstein et al.,* 1979; *Goldman et al.,* 1980]. This latter phenomenon involves a focusing effect in which the wave intensity increases in a region of decreased plasma density. Under the proper conditions the electric field pressure of the Langmuir wave causes the plasma density to decrease further, eventually forming an envelope soliton which collapses down to a spatial scale of only a few Debye lengths. Although some of these parametric decay and soliton collapse effects have been studied in the laboratory [*Wong and Quon,* 1975] and some indirect evidence exists for their occurrence in space plasmas [*Papadopoulos and Freund,* 1978], up to the present time none of these nonlinear effects have been directly observed in a space plasma. The purpose of this paper is to examine and analyze the interesting new Langmuir wave interactions observed by Voyager in the solar wind upstream of Jupiter's bow shock.

2. SURVEY OF OBSERVATIONS

The nonlinear Langmuir wave observations presented here were obtained during the Voyager 1 flyby of Jupiter in early March 1979. These data are unique in that an extremely high data rate, 115 kb/s, is available for sampling the electric field waveforms. See *Scarf and Gurnett* [1977] for a description of the instrument. This very high sampling rate allowed us to obtain very detailed electric field waveforms of Langmuir waves at frequencies extending well above the local electron plasma frequency, f_{pe}. During the approach to Jupiter, several intervals occurred in which intense beam-driven Langmuir waves were observed in the solar wind upstream of the bow shock [*Scarf et al.,* 1979*a*]. On the basis of our knowledge of similar waves observed upstream of the Earth's bow shock [*Scarf et al.,* 1971; *Gurnett and Frank,* 1975; *Filbert and Kellogg,* 1979] it is known that these waves are produced by electrons with energies of several keV escaping into the solar wind from the bow shock.

[1] Department of Physics and Astronomy, The University of Iowa, Iowa City, Iowa 52242.
[2] Research performed while on leave at the Institute of Geophysics and Planetary Physics, University of California, Los Angeles, California 90024.
[3] Institute of Geophysics and Planetary Physics, University of California, Los Angeles, California 90024.
[4] Space Science Department, TRW Defense and Space Systems Group, Redondo Beach, California 90278.

Paper number 80A1442.
0148-0227/81/080A-1442$01.00

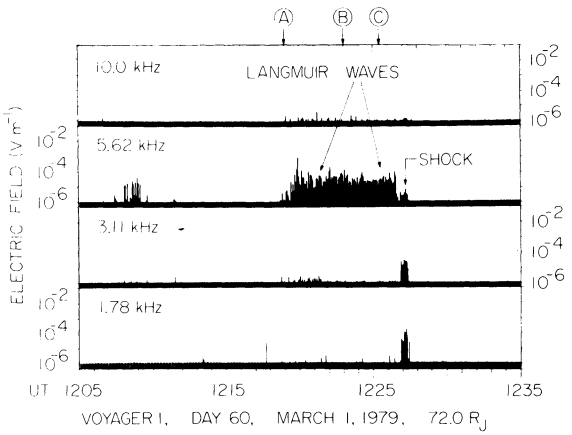

Fig. 1. The electric field intensities in four frequency channels showing the Langmuir wave emissions observed as Voyager 1 approaches Jupiter's bow shock on March 1, 1979.

The Langmuir waves associated with one of the bow shock crossings for which we have particularly good data are shown in Figure 1. This illustration gives the electric field intensity in four frequency channels near the electron plasma frequency, which at this time was approximately $f_{pe} = 5.6$ kHz. As can be seen from the abrupt burst of broadband noise in the 1.78- and 3.11-kHz channels, the shock is located at about 1227 UT. For a further discussion of this shock, see *Scarf et al.* [1979*b*]. The narrowband emissions in the 5.62-kHz channel upstream of the shock, from about 1218 to 1227 UT, are Langmuir waves generated by electrons streaming into the solar wind ahead of the shock. Although the exact energy of the peak in the electron energy spectrum cannot be determined from the Voyager data, the presence of energetic, ~15 keV, electrons arriving from the direction of the bow shock has been confirmed by the low-energy charged particle instrument on Voyager (S. M. Krimigis, personal communication, 1979). Since the beam was not detected by the Voyager plasma instrument (H. Bridge, personal communication, 1979), which is sensitive to electrons with energies up to 5.9 keV, the beam energy is probably between about 5.9 and 15 keV.

At this point it is useful to consider the electron beam geometry and the expected temporal evolution of the Langmuir wave emissions. Figure 2 shows a sketch of the magnetic field configuration which is thought to exist at the time of these observations. As determined from the Voyager magnetometer measurements (M. Acuna, personal communication, 1979), the magnetic field direction is at an angle of about 43° ± 5° with respect to the spacecraft-sun line during the event. From the results of *Filbert and Kellogg* [1979] it is known that the electron distribution function is determined by time-of-flight considerations from the point where the interplanetary magnetic field is tangent to the bow shock. Since the electrons escaping from the bow shock stream outward along the magnetic field, this condition gives a well defined sunward boundary to the beam. According to current understanding, the time-of-flight condition assures that an unstable double-humped velocity distribution is maintained throughout the region between the tangent field line and the bow shock. As soon as the approaching solar wind plasma contacts the escaping electron beam, Langmuir waves start to grow. Although the wave number $\mathbf{k}_0$, and group velocity $\mathbf{V}_g$, of these waves is directed along the magnetic field away from the shock, the group velocity is so small that the resulting wave packet is convected toward the shock with a velocity $\mathbf{V}_g' = \mathbf{V}_g + \mathbf{V}_{sw}$, as shown in Figure 2. Initially the wave grows exponentially at the linear growth rate. This linear growth region is evident in Figure 1 from about 1218 to 1220 UT. Eventually, however, nonlinear interactions limit the growth and the instability saturates. This nonlinear saturation region is evident in Figure 1 from the nearly constant electric field strength which exists from about 1220 to 1227 UT.

To illustrate the fine structure of the Langmuir waves, a series of frequency-time spectrograms of the wideband electric field waveforms are shown in Plate 1, near the beginning, middle, and end of the event, at points A, B, and C as indicated at the top of Figure 1. The red areas in these spectrograms indicate regions of relatively intense electric field strengths, blue areas indicate weak signals, and yellow and orange reflect intermediate field strengths, with a dynamic range of about 20 db from blue to red. The Langmuir wave emissions are clearly evident in these spectrograms as an intense narrowband emission centered at a frequency of about 5.6 kHz. This frequency is in close agreement with the local electron plasma frequency computed from the electron density, $n_e \simeq 0.45$ cm^{-3}, which was obtained from the Voyager plasma instrument (H. Bridge, personal communication, 1979). The

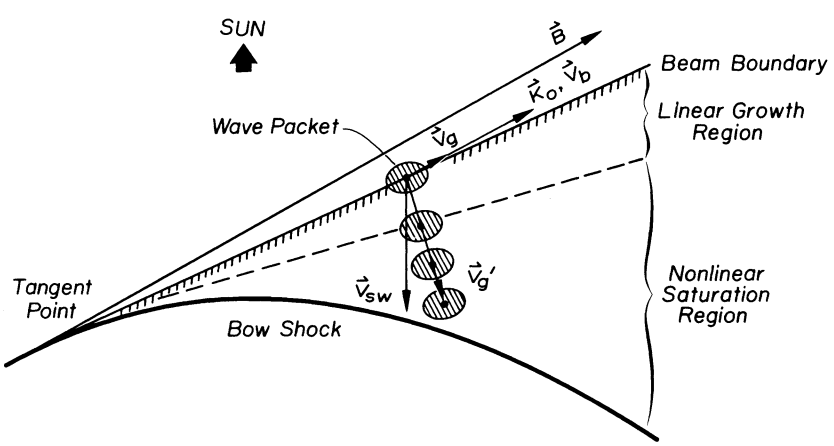

Fig. 2. A sketch of the magnetic field and electron beam geometry relevant for analyzing the Langmuir wave emissions shown in Figure 1. Wave packets excited by the electron beam are carried back toward the shock by the motion of the solar wind. The growth of the wave amplitude is expected to be divided into a linear growth region and a nonlinear saturation region. The boundary between these two regions is believed to occur at about 1220 UT in Figure 1.

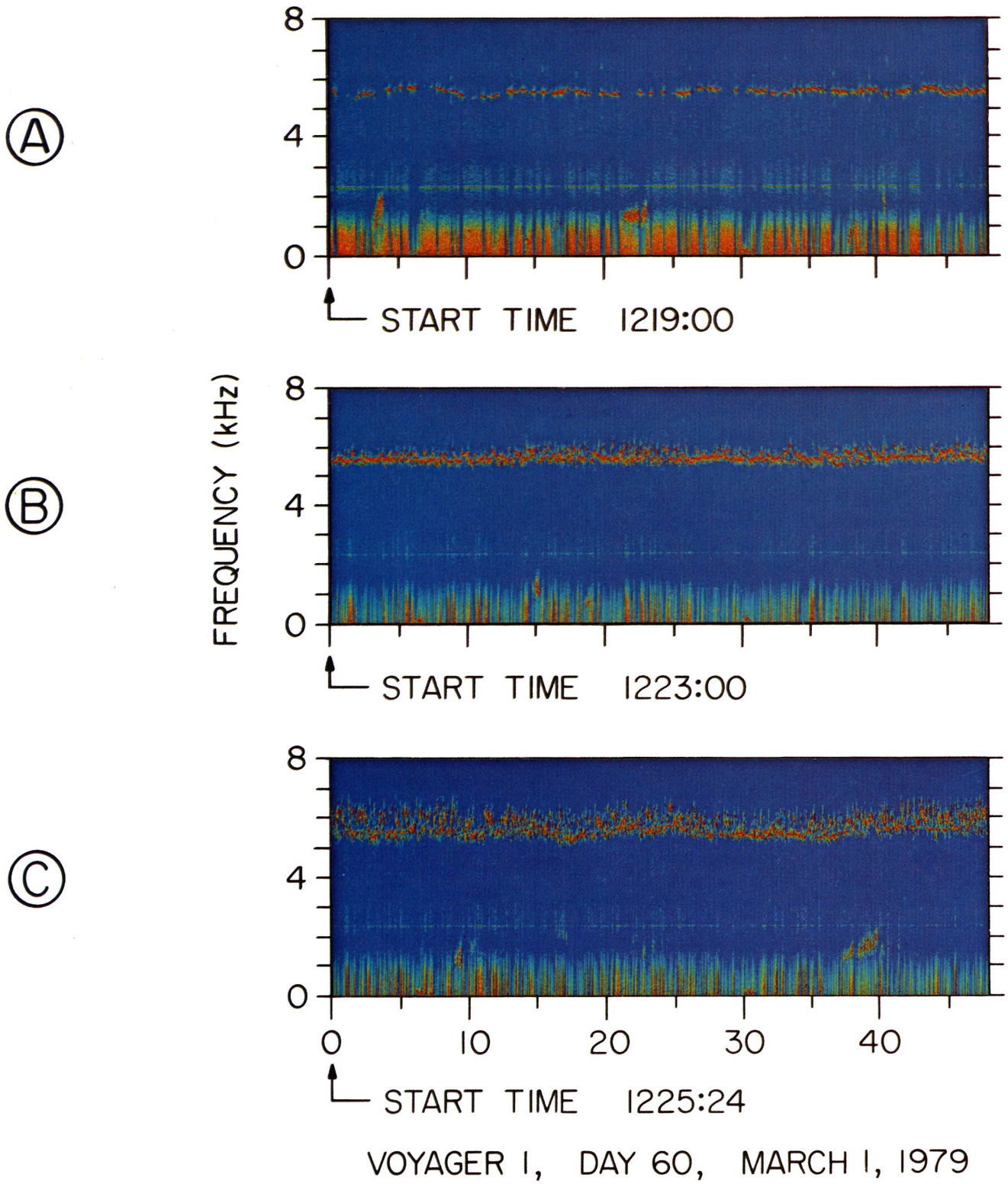

Plate 1. Frequency-time spectrograms from points A, B, and C in Figure 1. Red regions indicate large signal strengths, blue regions indicate small signal strengths, and intermediate amplitudes are represented by yellow and orange. Panel A is in the linear growth region and panels B and C are in the nonlinear saturation region. Strong sideband emissions, above and below the primary narrowband pump wave, are present throughout the nonlinear saturation region. These sideband emissions are believed to be the result of nonlinear interactions between the pump and the low frequency noise evident below about 500 Hz.

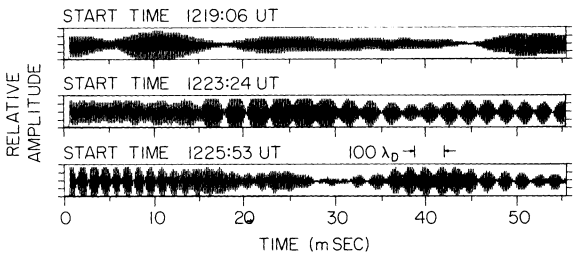

Fig. 3. Three representative electric field waveforms near the beginning, middle, and end of the event. Usually the sideband bursts have the appearance of a quasi-periodic amplitude modulation of the basic Langmuir wave emission, apparently resulting from the superposition of the sideband emission and the narrowband pump. The beat frequency tends to increase as the spacecraft approaches the shock, in agreement with the increasing frequency spread evident in Plate 1 from panel A to C.

nearly monochromatic emission at 2.4 kHz is an interference line produced by the spacecraft power supply. Other moderately intense plasma wave emissions, which will be discussed in greater detail later, can be seen at frequencies below about 2 kHz.

A striking feature of the Langmuir wave emissions in Plate 1 is the gradual transition from a nearly monochromatic spectrum at the onset of the event to a broad spiky spectrum as the spacecraft approaches the shock. For example, near the beginning of the event, in panel A of Plate 1, the bandwidth of the Langmuir wave emission is very narrow, less than 1%. Some fluctuations in the emission frequency are evident on time scales of several seconds or longer, however, these variations are believed to be caused by small scale density variations in the solar wind. Later, near the middle of the event, in panel B of Plate 1, the intense narrowband emission is still evident at f_{pe}, however, many brief bursts can now be seen extending both upward and downward from the main emission line. These discrete bursts continue to become more intense and spread in frequency until by the time the spacecraft reaches the shock, as in panel C of Plate 1, the Langmuir wave emission is almost completely broken up into many discrete bursts. The onset of the discrete bursts occurs at about 1220 UT, coincident with the transition from the linear growth region to the nonlinear saturation region. The maximum frequency spread of the Langmuir wave emission spectrum just ahead of the shock is about 1.2 kHz. As can be seen from Plate 1, the frequency spreading is quite asymmetrical with respect to the main emission line, with the upward frequency shift about a factor of three larger than the downward frequency shift.

Further high-time resolution details of the Langmuir wave emissions are illustrated in Figures 3 and 4. Figure 3 shows a selected sequence of electric field waveforms from near the beginning, middle, and end of the event. Although a wide variety of waveforms are observed these examples have been chosen to illustrate the most common feature, which consists of a nearly monochromatic burst with a quasi-periodic amplitude modulation. Usually the amplitude modulation pattern gives the impression of a beat between two signals of comparable amplitude. The beat frequency tends to increase as the spacecraft approaches the shock, consistent with the increasing frequency spread evident in Plate 1 at later and later times. Typically the individual bursts have durations of 50 to 200 ms, although as will be discussed later a few cases occur with durations as short as 10 ms. The fine structure of the individual bursts can be seen in greater detail in Figure 4 which shows an expanded frequency-time spectrogram of the interval just ahead of the shock. Usually the bursts consist of a sideband emission offset slightly above or below the main emission line. The linear superposition of the sideband and the main emission line appears to be responsible for quasi-periodic amplitude modulation pattern so prevalent in Figure 3. Although both upper and lower sideband emissions occasionally occur simultaneously, in most cases only one sideband emission is present at a time. Typically the sideband emission has a broader bandwidth and is more diffuse than the main emission line, which is very narrow and sharply defined. The sideband emissions also vary on a time scale much shorter than the main emission line, which tends to maintain a nearly constant amplitude for time scales of 500 ms or longer.

3. Evidence of Parametric Interactions

These observations of a strong main Langmuir wave emission line with upper and lower sidebands, together with the previously mentioned low frequency noise are strongly suggestive of a nonlinear parametric interaction. In this interpretation the main emission line is the beam-driven pump, and the sidebands and low frequency noise are the nonlinearly generated decay products. To further investigate this parametric decay process, it is important to establish the wavelength of the waves involved in the interaction. In order to relate the frequency spectrum of the Langmuir wave emissions to the wavelength we must consider both the intrinsic frequency variation caused by the dispersion relation and the Doppler shift caused by the motion of the solar wind. The dispersion relation for Langmuir waves is

$$f^2 = f_{pe}^2(1 + 3k^2\lambda_D^2) \tag{1}$$

where k is the wave number and λ_D is the Debye length. This dispersion relation is valid provided the weak turbulence condition, $E^2/8\pi nKT \ll (k\lambda_D)^2$, is satisfied [*Papadopoulos,* 1978]. Using $E \simeq 100$ μV/m from Figure 1 as a typical electric field strength, $n = 0.45$ cm^{-3} and $T = 3 \times 10^4$ °K from the Voyager plasma instrument (H. Bridge, personal communication, 1979), the dimensionless energy density ratio $E^2/8\pi nKT$ is approximately 2.3×10^{-7}. Since the instrument time constant of about 50 ms is shorter than the duration of most of the bursts this energy density ratio is valid for all except the very shortest bursts, which occur quite infrequently. Since, as will be shown, the wave number ratio $k\lambda_D$ is at least 10^{-2}, the weak turbulence condition is satisfied by nearly all of the bursts.

Using (1) and including the Doppler shift, the frequency shift with respect to the local plasma frequency, $\Delta f = f - f_{pe}$,

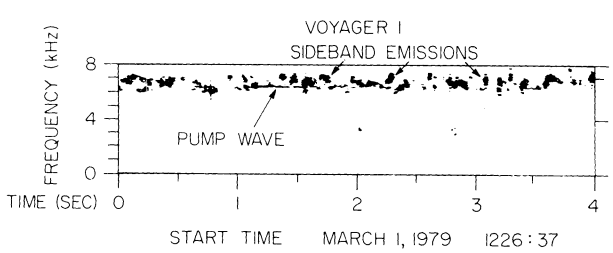

Fig. 4. An expanded frequency-time spectrogram showing the detailed structure of the sideband emissions. The sideband emissions are in general not symmetrical with respect to the main emission line. Usually only one sideband emission occurs at a time, suggesting that the main interaction is a three-wave process.

can be written

$$\Delta f = \left(\frac{V_{sw}}{2\pi\lambda_D}\right)(k\lambda_D)\cos\theta + f_{pe}\left\{-1 + [1 + 3(k\lambda_D)^2]^{1/2}\right\} \quad (2)$$

where V_{sw} is the solar wind velocity and θ is the angle between $\mathbf{k}$ and $\mathbf{V}_{sw}$. For the event being analyzed, the relevant parameters, as determined from the Voyager plasma measurements (H. Bridge, personal communication, 1979), are $V_{sw} = 420$ km/s, $f_{pe} = 5.6$ kHz, and $\lambda_D = 17.8$ m. Using these parameters the frequency shift is shown in Figure 5 as a function of $k\lambda_D$ for the limiting cases $\theta = 0°$ and $\theta = 180°$. These limiting cases, corresponding to waves propagating away from and toward the sun, give upper and lower bounds to the frequency spectrum.

To analyze the frequency spectrum, we first consider the frequency shift of the beam-driven pump wave. For a beam of velocity V_b it is easily shown [*Krall and Trivelpiece,* 1973] that the wave number excited by the beam is approximately $k_0\lambda_D = V_e/V_b$, where V_e is the electron thermal speed. Using the measured electron thermal energy of 2.75 eV and an estimated beam energy of 10 keV, $k_0\lambda_D$ is estimated to be approximately 0.016. Referring to Figure 5, it is seen that the frequency shift of the pump wave is very small, only about 60 Hz. The pump wave, which corresponds to the nearly continuous main emission line in Plate 1, is therefore essentially at the local electron plasma frequency. It is clear from examination of Figure 5 that to account for the large frequency shift of the sideband emissions, these emissions must have wave numbers much larger than the pump. For moderately small wave numbers, $k\lambda_D < 0.5$, positive frequency shifts correspond to waves propagating away from the sun and negative frequency shifts correspond to waves propagating toward the sun. The wavelength of the parametrically generated forward and backward propagating waves can be estimated from the observed frequency spreading. As can be seen from Figure 5, the maximum negative frequency shift which can be obtained for the sunward propagating ($\theta = 180°$) waves is about 400 Hz. This frequency shift is in good agreement with the maximum frequency shift evident for the lower sideband emissions in panel C of Plate 1, which is typically about 300 Hz. This close agreement indicates that some of the sunward propagating waves have normal directions near $\theta \simeq 180°$ with wave numbers at least as large as $k\lambda_D \simeq 0.15$. The exact limit to $k\lambda_D$ cannot be accurately determined for the sunward propagating waves because of the double valued dependence of the frequency shift on the wave number. The exact range of wave normal angles is also quite uncertain because of the weak dependence of Δf on θ near 180°. The frequency shift would, for example, be consistent with propagation directly along the interplanetary magnetic field (i.e., parallel to the electron beam). For the antisunward propagating waves the wave number can be estimated in a similar manner using Figure 5. From panel C of Plate 1 it is seen that the maximum frequency shift for the upper sideband is about 900 Hz. For a wave normal angle of $\theta = 0°$, Figure 5 shows that the corresponding upper limit to the wave number for the antisunward propagating waves is about $k\lambda_D = 0.16$. If the wave normal angle is changed to $\theta_B = 43°$ (i.e., propagation parallel to the electron beam), the upper limit to the wave number increases slightly, to about $k\lambda_D = 0.18$.

This analysis shows that the original rather small wave number of the pump wave, with $k_0\lambda_D \simeq 0.016$, is very efficiently converted into both forward and backward propagating waves with much larger wave numbers, up to $k\lambda_D \simeq 0.15$. In considering the possible parametric processes which could produce this conversion it is important to identify the low frequency wave mode involved in the interaction. From inspection of the spectrograms in Plate 1 it is clear that substantial wave intensities are present at frequencies below about 2 kHz. Two types of emissions can be identified in this frequency range. First, there are a few sporadic bursts of narrowband ion-acoustic waves of the type discussed by *Kurth et al.* [1979]. These bursts are evident, for example, at about 3 and 22 s in panel A of Plate 1. Since these bursts occur quite infrequently and do not appear to have any obvious temporal correspondence to the Langmuir wave bursts, it seems very unlikely that these waves play any role in the Langmuir wave decay. A second type of emission, increasing in intensity with decreasing frequency, is also evident in the spectrograms of Plate 1 at frequencies below about 500 Hz. Although this type of noise has not been previously identified in the solar wind, it seems quite likely that it also consists of some type of low frequency electrostatic mode, again possibly ion-acoustic waves. The spectrum of the low frequency noise is illustrated in more detail in Figure 6, which shows a sequence of electric field spectrums separated by 60 ms starting at 1226:06.44 UT, near the end of panel C in Plate 1. This illustration shows that the low frequency noise spectrum changes dramatically on a time scale of 60 ms or less, on approximately the same time scale as the variations in the Langmuir wave emissions. Since all of the known low frequency electrostatic modes of propagation have phase velocities much smaller than the solar wind velocity, it is almost certain that the frequency spectrum measured in the spacecraft frame of reference is determined by Doppler shifts. If we use 500 Hz as the approximate upper frequency limit of the low frequency noise spectrum, then the maximum wave number of the low frequency noise would be approximately $k_L\lambda_D = 2\pi f_{max}\lambda_D/V_{sw} \simeq 0.14$. This wave number is approximately the same as the maximum wave number of the sideband emissions. The close similarity of the two wave numbers provides strong evidence that the low frequency waves are involved in parametric interactions with the Langmuir waves since if the pump wave number k_0 is very small, as is

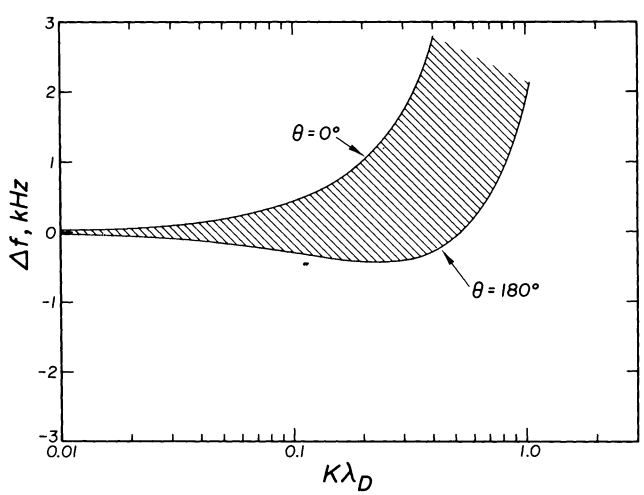

Fig. 5. The frequency shift relative to the electron plasma frequency as a function of the normalized wave number $k\lambda_D$ for the parameters relevant to the event in Plate 1. To account for the observed bandwidth of the sideband emissions, wave numbers up to approximately $k\lambda_D \simeq 0.15$ must be present.

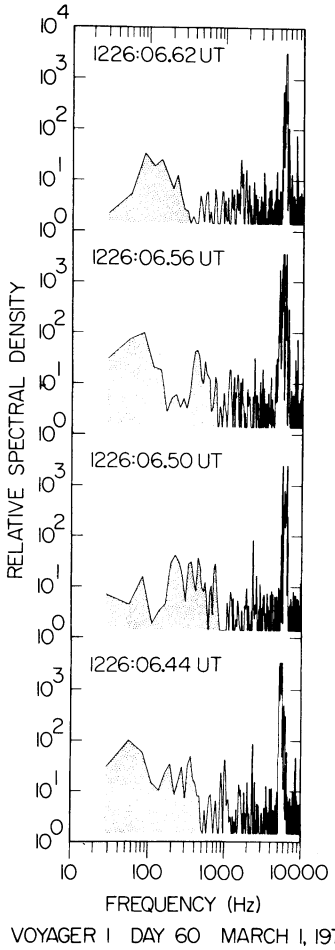

Fig. 6. A sequence of frequency spectrums separated by only 60 ms showing the rapid and somewhat similar changes in the spectrum of the low frequency noise (shaded) and the Langmuir wave sideband structure.

the case, then conservation of momentum

$$\mathbf{k} = \mathbf{k}_0 + \mathbf{k}_L \tag{3}$$

shows that $|\mathbf{k}| \simeq |\mathbf{k}_L|$, which is to a good approximation satisfied.

Further evidence on the mode of propagation of the low frequency noise can be obtained from the conservation of energy relation, which is

$$f = f_0 + f_L \tag{4}$$

Since the maximum wave number of the sideband emissions is known, $k\lambda_D \lesssim 0.15$, and the frequency of the pump wave is very close to the electron plasma frequency, $f_0 \simeq f_{pe}$, the upper frequency limit for the low frequency mode can be estimated from (4):

$$f_L \lesssim f_{pe}[1 + 3(k\lambda_D)^2]^{1/2} - f_{pe} \tag{5}$$

which gives $f_L \lesssim 186$ Hz. This upper frequency limit is very close to the ion plasma frequency $f_{pi} \simeq 130$ Hz, which provides a strong indication that the low frequency noise consists of ion-acoustic waves since ion-acoustic waves can propagate up to frequencies near the ion plasma frequency.

Although it seems reasonably certain from the above comparisons that the low frequency noise is involved in nonlinear interactions with the Langmuir wave spectrum, it is not clear to what extent the low frequency noise is generated or enhanced by the presence of the Langmuir wave emissions. Detailed examination of the low frequency noise spectrum shows that this noise is present to some extent even when the Langmuir waves are absent. In fact, it is our impression from examination of the Voyager waveform data that a low level of ion-acoustic-like turbulence is present much of the time in the solar wind. At the present time we do not have any explanation for the origin of this noise. The integrated broadband electric field strength of this noise is very small, only about 3 to 10 μV m^{-1}. Even though these waves are quite weak, the intensities are still much larger than the thermal level of ion-acoustic fluctuations which would be expected in the solar wind.

4. Interaction Mechanisms

When comparing the Voyager Langmuir wave observations with existing theories for nonlinear beam-plasma interactions, one is faced with a number of interpretive problems, some of which may not be immediately resolvable without further study and investigation. In general, nonlinear beam-plasma interactions can be divided into two regimes, called weak and strong turbulence, which are characterized by the dimensionless electric field energy density ratio $W/nKT = E^2/8\pi nKT$. If $W/nKT < (k_0\lambda_D)^2$, then the linear dispersion relation given by (1) is valid and the evolution of the wave and particle spectrums are describable by quasi-linear theory (for example, see *Krall and Trivelpiece* [1973]). On the other hand, if $W/nKT \geq (k_0\lambda_D)^2$, then the resulting interactions are usually described in terms of the oscillating two stream (OTS) instability [*Papadopoulos et al.,* 1974] or the fully nonlinear phenomena of soliton formation and collapse [*Nicholson et al.,* 1978]. In the present case we seem to have a curious combination of both weak and strong turbulence effects. The electric field strength shows that for all but a few isolated bursts, which are discussed in the next section, the Langmuir wave intensities are sufficiently small, $W/nKT \ll (k_0\lambda_D)^2$, to be regarded as weak turbulence. For weak turbulence, however, the direction of nonlinear energy transfer is toward smaller wave numbers [*Papadopoulos,* 1978], rather than toward larger wave numbers as is observed. In general, except for the threshold electric field strength, most of the characteristics of the Langmuir waves observed by Voyager are in agreement with the expectations of strong turbulence theory. For example, the OTS instability provides a mechanism for transferring energy toward larger wave numbers, in agreement with the Voyager observations. Furthermore, computer simulations [*Papadopoulos and Freund,* 1978] of the OTS show that the energy in the beam-driven pump wave is rapidly transferred to wave numbers near $k\lambda_D \simeq 0.2$, in close quantitative agreement with estimated wave number of the sideband structure observed by Voyager. Although the early analyses of the OTS by *Papadopoulos et al.* [1974] and others using the dipole ($k_0\lambda_D \simeq 0$) approximation indicate a symmetrical sideband structure in disagreement with the Voyager observations, various processes such as a finite pump wave number can lead to marked asymmetries in the sideband structure, thereby possibly accounting for the fact that the upper and lower sideband emissions usually do not occur simultaneously (see Figure 4).

Since the main difficulty with the strong turbulence interpretation has to do with the threshold field strength at which nonlinear effects become important, it is useful to consider mechanisms which could modify this threshold. One possible

mechanism for lowering the OTS threshold is the prior existence of a nonthermal level of low frequency density fluctuations [*Smith et al.*, 1979]. Since the Voyager observations apparently indicate the nearly continuous presence of a low level of ion-acoustic-like fluctuations in the solar wind, the possibility exists that the threshold for the OTS instability could be substantially reduced. The observed density fluctuations are quite small, however, with $\delta n/n \simeq 10^{-4}$ if the fluctuations are due to ion-acoustic waves. *Smith et al.* [1979] estimate that ion fluctuations begin to significantly affect the OTS threshold when $\delta n/n \gtrsim 3(k\lambda_D)^2 \simeq 10^{-3}$. It remains to be seen whether the observed fluctuations can cause a significant reduction in the OTS threshold.

Because of the prior existence of a background of ion-acoustic-like fluctuations in the solar wind, another possible interpretation is that the sideband structure is simply the consequence of three-wave scattering involving the beam-driven pump wave, the sideband emission and the nonthermal ion-acoustic waves. This three wave scattering mechanism differs fundamentally from the parametric decay mechanisms described above in that the energy for the ion-acoustic waves is not derived from the Langmuir waves. One difficulty with the scattering mechanism is that scattering by itself does not provide a local nonlinear stabilization mechanism to account for the saturation effect evident in Figure 1. However, other processes, such as spatial variations in the beam resonance condition, could also be invoked to limit the electric field amplitudes.

Simple considerations involving conservation of energy and momentum for Langmuir wave interactions with ion-acoustic waves show that the maximum wave number change per interaction is $\Delta k\lambda_D \simeq 2/3(m_e/m_i)^{1/2} = 0.016$. Since wave numbers as large as $k\lambda_D = 0.15$ are observed, it is evident that several interactions would be necessary to reach such large wave numbers. The fact that several interactions are required does, however, provide a simple explanation for the monotonic increase in the bandwidth of the sideband emissions as the spacecraft approaches the shock. Since the number of interactions is expected to grow linearly with time, the spread in the wave number of the scattered Langmuir waves and the corresponding spread in the frequency spectrum of the sideband emissions should increase more or less linearly with time as is observed.

The scattering rate for long wavelength plasmons off low frequency electrostatic ion waves with intensity levels above thermal is given by *Smith et al.* [1979] as

$$\gamma \simeq \left(\frac{\pi}{2}\right) \frac{\omega_p}{(k\lambda_D)^2} \left(\frac{\delta n}{n}\right)^2 \tag{6}$$

where δn is the root-mean-square density fluctuation due to the ion waves. An estimate of δn can be obtained from the total low frequency electric field strength by using the relation valid for an ion-acoustic wave of wave number $\mathbf{k}$,

$$\frac{\delta n}{n} = \frac{eE}{KT_e k} \tag{7}$$

From Figure 6 it can be seen that the characteristic, or peak, frequency for the low frequency ion noise is approximately 100 Hz which corresponds to a wave number of $k\lambda_D \simeq 3 \times 10^{-2}$. Using this value of k and a total broadband field strength of 10 μV/m for the ion noise, the density fluctuation found from (7) is $\delta n/n = 2 \times 10^{-4}$. Using (6), this gives a scattering rate of about 0.5 s^{-1}, which corresponds to an average scattering time of about 2 s. This scattering time must be compared with the duration of the interaction in the plasma frame of reference. If we assume that the shock is stationary, then for the known spacecraft and solar wind velocities the duration of the event in the solar wind frame of reference is estimated to be about 16 to 20 s. The estimated scattering rate is therefore more than adequate to account for the number of multiple interactions required to explain the observed spread in the wave number spectrum.

5. Evidence of Collapsed Wave Packets

Although the temporal structure of the Langmuir wave emissions usually consists of amplitude modulated wave trains lasting 50 ms or more, as in Figure 3, occasionally very intense isolated bursts occur lasting only a few milliseconds. Three examples of these very short duration bursts are shown in Figure 7. As can be seen, these bursts consist of isolated nearly monochromatic wave packets with durations of only about 5 to 10 ms, corresponding to only 15 to 30 plasma oscillation periods. Bursts of this type sometimes occur individually and sometimes as a loosely organized sequence of several bursts. The bursts are often very intense and frequently saturate the receiver, causing a clipped sine wave. Short intense bursts of this type tend to occur most frequently later in the event, after the pump wave has almost completely broken up into many discrete emissions, as in panel C of Plate 1. Since the group velocity is much less than the solar wind velocity, the approximate spatial size of a packet can be estimated from the time it takes the packet to sweep by the spacecraft. An approximate spatial scale is shown in Figure 7 in units of the Debye length. The wave packets in this case have a scale size of about $100\lambda_D$. Typically the scale size of these intense wave packets ranges from about $50\lambda_D$ to $500\lambda_D$.

These observations of intense isolated wave packets with scale sizes of 50 to 100 Debye lengths are very suggestive of the formation of collapsed envelope solitons of the type described by *Zakharov* [1972], *Galeev et al.* [1975], *Nicholson et al.* [1978], and others. The crucial question of whether these wave packets are collapsing solitons or not involves the electric field strength. The occurrence of solitions via strong nonlinear interactions implies electric field intensities on the order

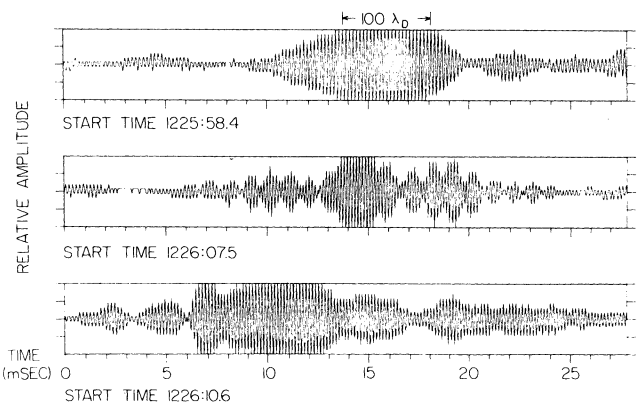

Fig. 7. The electric field waveforms of three Langmuir wave bursts of unusually short duration. These bursts consist of very intense wave packets which have collapsed down to a spatial scale of only a few Debye lengths.

of

$$\frac{E^2}{8\pi nKT} \geq (\Delta k \lambda_D)^2 \tag{8}$$

where nKT is the electron energy density and Δk is a wave number characteristic of the envelope (see, for example, *Thornhill and ter Haar* [1978]). Using $\Delta k = 2\pi/L$, with $L = 100\lambda_D$ as a typical scale length, $n = 0.45$ cm^{-3}, and $T = 3 \times 10^4$ °K, the electric field strength necessary for soliton formation is estimated to be about 12.8 mV m^{-1}.

Unfortunately, it is very difficult to accurately determine the field strength of these short very impulsive bursts. The only absolute field strength measurements available are from the spectrum analyzer measurements in Figure 1 which indicate field strengths of 0.1 to 0.3 mV m^{-1}. These field strength measurements are an average of the logarithm of the electric field intensities with an averaging time constant of 50 ms. Although this time constant is short enough to provide accurate measurements of the longer duration wave trains of the type shown in Figure 3, it is too long to resolve the short duration bursts of the type shown in Figure 7. For bursts as short as 10 ms the field strengths can be underestimated by a large factor, possibly as much as 10^2 to 10^3. To make a rough estimate of the peak electric field intensity, we have played the recorded waveform signals through a spare version of the Voyager plasma wave instrument and adjusted the waveform amplitude such that the output of the 5.62-kHz channel has a value comparable to the saturation level in Figure 1. Based on these tests it appears that at least some of the peak electric field strengths exceed 1 mV m^{-1}. This simultation has the shortcoming that since the most intense bursts are usually severely clipped, there is no way to determine by what factor some of the signals may have exceeded 1 mV m^{-1}. Based on the absence of certain receiver distortion effects which occur for very large field strengths, we can place an upper limit to the maximum field strength of about 50 mV m^{-1}. Unfortunately, the resulting limit on the peak electric field strength of the bursts, 1 mV m^{-1} $< E <$ 50 mV m^{-1}, does not provide conclusive evidence that these wave packets consist of collapsing solitons. The best that can be concluded is that the peak electric field strengths are within a factor of 10 of the soliton collapse threshold.

6. Discussion

In this paper we have used the very high resolution waveform measurements available from the Voyager plasma wave instrument to investigate the nonlinear stabilization of beam-driven Langmuir wave emissions observed in the solar wind upstream of the Jovian bow shock. The primary characteristic of the observed nonlinear interactions involves the generation of very spiky sideband emissions on either side of the main beam-driven pump wave. This sideband structure has been interpreted as being due to parametric interactions of the beam-driven Langmuir waves with a preexisting background of ion-acoustic wave turbulence which is apparently always present in the solar wind. Positive frequency shifts arise from waves propagating backward away from sun and the negative frequency shifts arise from waves propagating forward toward the sun. The magnitude of the frequency shifts shows that the long wavelength pump wave is being very efficiently converted into short wavelength Langmuir waves, $k\lambda_D \simeq 0.15$, which are no longer in resonance with the beam. Evidence that this parametric interaction stabilizes the beam is provided by the fact that the sideband emissions first appear at about the time that the amplitude of the pump wave saturates. Detailed examination of the electric field waveforms shows a very complex structure, including the occasional occurrence of very intense wave packets on spatial scales of 50 to $500\lambda_D$. These very small scale structures are thought to be envelope solitons which have collapsed down to spatial scales of a few Debye lengths.

One puzzling aspect of these Langmuir wave interactions is the apparent occurrence of strong turbulence effects (energy conversion to larger wave numbers) even though the average field strengths are in the weak turbulence regime. The apparent decrease in the threshold for strong turbulence effects may be closely related to the presence of the low level of ion-acoustic-like turbulence which is nearly always present in the solar wind. Although the background ion-acoustic wave turbulence observed during this event is quite weak, only about 10 μV m^{-1}, it is still much larger than the thermal level which is usually assumed in most modulational instability analyses. Although some theoretical work has been done on the effect of nonthermal density fluctuations on the threshold for strong turbulence processes such as the OTS instability [*Smith et al.*, 1979], additional work is still needed to see if the threshold reduction caused by the background ion-acoustic turbulence can be reconciled with the low field strengths observed. Although not much is known about the origin and characteristics of the background ion-acoustic noise, it is our present impression that this noise is essentially a permanent feature of the solar wind since it has been observed in every case for which we have wideband data. Further studies are clearly needed to establish the characteristics of this noise as a function of radial distance from the sun before the implications for the propagation of energetic solar electrons can be fully evaluated.

The observation of intense packets of Langmuir waves with spatial sizes of only $100\lambda_D$, or less provides possibly the first observations of collapsed Langmuir wave solitons in a space plasma. The principal uncertainty in identifying these intense wave packets as solitons is that the maximum electric field strength cannot be determined with good accuracy on such short time scales. The observations show that the electric field strengths are within a factor of 10 of the threshold needed for soliton collapse, and may very well exceed this threshold. Further more detailed studies are being planned to try to provide a better determination of the electric field strength and to investigate other characteristics, such as the frequency shift within the packet, which may provide a more definitive identification of the nonlinear process responsible for these bursts.

Acknowledgments. The authors would like to express their thanks to K. Papadopoulos, M. Goldstein, D. Nicholson, G. Morales, and C. Kennel for their helpful comments and suggestions during the preparation of this manuscript. The research at the University of California was supported by the National Science Foundation through grant ATM-78-19958. The research at The University of Iowa was supported by the National Aeronautics and Space Administration through grants NGL-16-001-002 and NGL-16-001-043 from NASA Headquarters, through contract 954013 with the Jet Propulsion Laboratory, and by the Office of Naval Research. The research at TRW was supported by NASA through contract 954012 with the Jet Propulsion Laboratory.

REFERENCES

Bardwell, S., and M. V. Goldman, Three-dimensional Langmuir wave instabilities in type III solar radio bursts, *Astrophys. J., 209,* 912, 1976.

Bohm, D., and E. P. Gross, Theory of plasma oscillations: A, Origin of medium-like behavior; B, Excitation and damping of oscillations, *Phys. Rev., 75,* 1851, 1949.

Filbert, P. C., and P. J. Kellogg, Electrostatic noise at the plasma frequency beyond the bow shock, *J. Geophys. Res., 84,* 1369, 1979.

Freund, H. P., and K. Papadopoulos, Oscillating two-stream and parametric decay instability in a weakly magnetized plasma, *Phys. Fluids, 23,* 139, 1980.

Fried, B. D., T. Ikemura, K. Nishikawa, and G. Schmidt, Parametric instabilities with finite wavelength pump, *Phys. Fluids, 19,* 1975, 1976.

Galeev, A. A., R. Z. Sagdeev, Yu. S. Sigov, V. D. Shapiro, and V. I. Shevchenko, Nonlinear theory for the modulation instability of plasma waves, *Sov. J. Plasma Phys. Engl. Transl., 1,* 5, 1975.

Goldman, M. V., G. F. Reiter, and D. R. Nicholson, Radiation from a strongly turbulent plasma: Application to electron beam–excited solar emissions, *Phys. Fluids, 23,* 388, 1980.

Goldstein, M. L., R. A. Smith, and K. Papadopoulos, Nonlinear stability of solar type III radio bursts, II, Application to observations near 1 AU, *Astrophys. J., 234,* 683, 1979.

Gurnett, D. A., and L. A. Frank, Electron plasma oscillations associated with type III radio emissions and solar electrons, *Solar Phys., 45,* 477, 1975.

Kaplan, S. A., and V. N. Tsytovich, Radio emission from beams of fast particles under cosmic conditions, *Sov. Astron. Engl. Transl., 11,* 956, 1968.

Krall, N., and A. Trivelpiece, *Principles of Plasma Physics,* 460 pp., McGraw-Hill, New York, 1973.

Kurth, W. S., D. A. Gurnett, and F. L. Scarf, High-resolution spectrograms of ion acoustic waves in the solar wind, *J. Geophys. Res., 84,* 3413, 1979.

Lin, R. P., The emission and propagation of ~40 keV solar flare electrons, *Solar Phys., 12,* 266, 1970.

Nicholson, D. R., M. V. Goldman, P. Hoyng, and J. C. Weatherall, Nonlinear Langmuir waves during type III solar radio bursts, *Astrophys. J., 223,* 605, 1978.

Papadopoulos, K., On the physics of strong turbulence for electron plasma waves, in *Proceedings of the Varenna School on Plasma Physics,* p. 355, Pergamon, New York, 1978.

Papadopoulos, K., and H. P. Freund, Solitons and second harmonic radiation in type III bursts, *Geophys. Res. Lett., 5,* 881, 1978.

Papadopoulos, K., M. L. Goldstein, and R. A. Smith, Stabilization of electron streams in type III solar radio bursts, *Astrophys. J., 190,* 175, 1974.

Sagdeev, R. Z., and A. A. Galeev, *Nonlinear Plasma Theory,* W. A. Benjamin, New York, 1969.

Scarf, F. L., and D. A. Gurnett, A plasma wave investigation for the Voyager mission, *Space Sci. Rev., 21,* 289, 1977.

Scarf, F. L., R. W. Fredricks, L. A. Frank, and M. Neugebauer, Nonthermal electrons and high-frequency waves in the upstream solar wind, 1, Observations, *J. Geophys. Res., 76,* 5162, 1971.

Scarf, F. L., D. A. Gurnett, and W. S. Kurth, Jupiter plasma wave observations: An initial Voyager 1 overview, *Science, 204,* 991, 1979*a*.

Scarf, F. L., D. A. Gurnett, W. S. Kurth, and R. L. Poynter, Plasma wave turbulence at Jupiter's bow shock, *Nature, 280,* 796, 1979*b*.

Smith, R. A., M. L. Goldstein, and K. Papadopoulos, Nonlinear stability of solar type III radio bursts, I, Theory, *Astrophys. J., 234,* 348, 1979.

Thornhill, S. G., and D. ter Haar, Langmuir turbulence and modulational instability, *Phys. Rep., 43,* 43, 1978.

Wong, A. Y., Electromagnetic wave interactions with inhomogeneous plasmas, in *Laser Interaction and Related Plasma Phenomena,* edited by H. Schwarz and H. Hora, p. 783, Plenum, New York, 1977.

Wong, A. Y., and B. H. Quon, Spatial collapse of beam-driven plasma waves, *Phys. Rev. Lett., 34,* 1499, 1975.

Zakharov, V. E., Collapse of Langmuir waves, *Sov. Phys. JETP Engl. Transl., 35,* 908, 1972.

(Received February 19, 1980;
revised September 30, 1980;
accepted October 10, 1980.)